Journal of Power Sources 195 (2010) 4114–4118

Contents lists available at ScienceDirect

Journal of Power Sources

journal homepage: www.elsevier.com/locate/jpowsour

Short communication

Performance and durability of nanostructured $(La_{0.85}Sr_{0.15})_{0.98}MnO_3$/yttria-stabilized zirconia cathodes for intermediate-temperature solid oxide fuel cells

Kazuyoshi Sato[a,*], Toru Kinoshita[b], Hiroya Abe[a]

[a] Joining and Welding Research Institute, Osaka University, 11-1 Mihogaoka, Ibaraki, Osaka 567-0047, Japan
[b] New Technology Research Laboratory, Sumitomo Osaka Cement Co., Ltd., 585 Toyotomi-Cho, Funabashi, Chiba 247-8601, Japan

ARTICLE INFO

Article history:
Received 11 November 2009
Received in revised form
22 December 2009
Accepted 21 January 2010
Available online 25 January 2010

Keywords:
Solid oxide fuel cells
LSM/YSZ cathode
Nanostructure
Power density
Durability

ABSTRACT

In this communication we report the fabrication of nanostructured $(La_{0.85}Sr_{0.15})_{0.98}MnO_3$ (LSM)/yttria-stabilized zirconia (YSZ) composite cathodes consisting of homogeneously distributed and connected LSM and YSZ grains approximately 100 nm large. We also investigate for the first time the role of the cathode nanostructure on the performance and the durability of intermediate-temperature solid oxide fuel cells. The cathodes were fabricated using homogenous LSM/YSZ nanocomposite particles synthesized by co-precipitation, using YSZ nanoparticles of 3 nm as seed crystals. Detailed microstructural characterization by transmission electron microscopy with energy-dispersive X-ray spectroscopy revealed that many of the LSM/YSZ junctions in the cathode faced the homogeneously connected pore channels, indicating the formation of a considerable number of triple phase boundaries. The nanostructure served to reduce cathodic polarization. As a result, these anode-supported solid oxide fuel cells showed high power densities of 0.18, 0.40, 0.70 and 0.86 W cm^{-2} at 650, 700, 750 and 800 °C, respectively, under the cell voltage of 0.7 V. Furthermore, no significant performance degradation of the cathode was observed during operation at 700 °C for 1000 h under a constant current density of 0.2 A cm^{-2}.

1. Introduction

Strontium-doped lanthanum manganite $(La_xSr_{1-x})_yMnO_3$ (LSM)/yttria-stabilized zirconia (YSZ) composite is a promising cathode material for solid oxide fuel cells (SOFCs) operated at 900 °C or higher. Recent research and development on SOFCs have been directed to reduce the operation temperature into the so-called intermediate range (650–800 °C), with the aim of cost reduction and durability enhancement of the cells and the system. In this temperature range, however, the oxygen reduction reaction (ORR) property of the cathode often limits the overall performance of the state-of-the-art SOFCs with a Ni/YSZ cermet anode, thin YSZ electrolyte and LSM/YSZ composite cathode [1]. Previous studies on the relationship between microstructure and performance of the composite cathode have shown that ORR occurs in the vicinity of triple phase boundaries (TPBs), where LSM, YSZ and pore phases meet [2–4]. These pioneering studies have stimulated considerable efforts in optimizing cathode microstructure for improved performance [5–8]. Recently, Wang et al. reported that the performance of intermediate-temperature SOFC (IT-SOFC) can be significantly improved by reducing the grains of the composite cathode from conventional micron size down to 100 nm [9].

Long-term stability is another important requirement of fuel cell technology. It has been reported recently that performance degradation of the LSM/YSZ cathode often dominates that of the IT-SOFCs and becomes significant rather at lower temperatures [10–12]. Liu et al. have reported that the degradation can be attributed to the formation of zirconates ($La_2Zr_2O_7$ and $SrZrO_3$) related to the chemical instability of LSM under a current load [11]. Their thermodynamic calculations suggested that the high performance LSM/YSZ cathode could suppress the formation of zirconates, thereby improving long-term stability of the cells. Furthermore, Song et al. have demonstrated that a cathode with uniformly distributed LSM and YSZ shows better long-term stability than that with a nonuniform microstructure [8].

Based on previous reports [8–12], we can predict that homogeneous nanostructured cathodes with fine LSM and YSZ grains of smaller than 100 nm are promising candidates for IT-SOFC cathodes. The nanostructure of the cathodes should be optimized not only to enhance performance, but also to maximize long-term stability. Therefore, the role of nanostructure in performance and durability must be well understood; however, it has thus far remained unclear, possibly due to the difficulty of fabrication of the nanostructured cathodes. Actually, no nanostructured cathodes

* Corresponding author. Tel.: +81 668 79 4370; fax: +81 668 79 4370.
E-mail address: k-sato@jwri.osaka-u.ac.jp (K. Sato).

0378-7753/$ – see front matter © 2010 Elsevier B.V. All rights reserved.
doi:10.1016/j.jpowsour.2010.01.045

have been reported in the literature after a report by Wang et al. [9]. For fabrication of a homogeneous nanostructured cathode using conventional particle processing, it is necessary to synthesize the starting particles, which consist of homogeneously distributed LSM and YSZ particles much smaller than 100 nm, taking into account grain growth during sintering. Virtually all LSM/YSZ composite cathodes to date can be described as a physical mixture of separately synthesized LSM and YSZ particles. However, the possible particle size for uniform mixing is above sub-micron [5], hence the grain size of the resultant cathodes is typically on the order of one to several microns. Although there are few reports on the synthesis of LSM/YSZ nanocomposite particles by build-up methods [6–8], significant grain growth during the post-sintering process resulted in sub-micron grain size. This may be due to the lack of homogeneity in the size and distribution of LSM and YSZ phases.

We have recently successfully synthesized homogeneous $(La_{0.85}Sr_{0.15})_{0.98}MnO_3$/YSZ nanocomposite particles through a novel co-precipitation method using 3-nm diameter YSZ nanoparticles as seed crystals. The cathode fabricated by nanocomposite particles consisted of grains approximately 100 nm in size. In the present study, we analyze the detailed nanostructure of these cathodes and investigate the role of nanostructure on the performance and durability of IT-SOFCs.

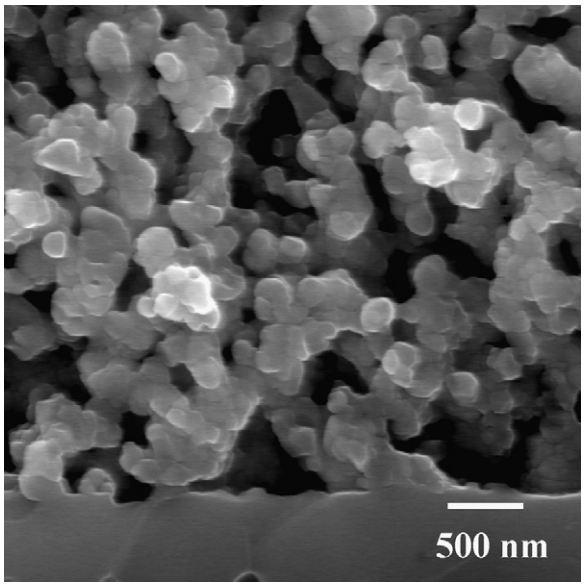

Fig. 1. A cross-sectional SEM image of the cathode/electrolyte interface of the anode-supported cell.

2. Experimental

Anode-supported and symmetric cells were fabricated using $(La_{0.85}Sr_{0.15})_{0.98}MnO_3$/YSZ nanocomposite particles. The mass fraction of LSM and YSZ in the nanocomposite was even. The detailed synthesis procedure of the composite particles was described in the previous report [13]. The anode-supported cell was fabricated in manner similar to previous studies [14,15]. Thin YSZ electrolyte (approximately 10 μm thick)/thick NiO/YSZ anode (approximately 500 μm thick) bi-layer was fabricated by tape casting, followed by co-sintering at 1350 °C for 2 h. A cathode layer 6 mm in diameter was deposited onto the thin film YSZ electrolyte by screen printing, followed by sintering at 1100 °C for 2 h. Symmetric cells were fabricated in the following manner. First, a dense YSZ electrolyte disk 13 mm in diameter and 450 μm in thickness was fabricated by tape casting, followed by sintering at 1350 °C for 2 h. Second, an LSM/YSZ layer 6 mm in diameter was deposited symmetrically on both sides of the YSZ disk using the conditions above. Platinum paste 2 mm in diameter was applied onto the counter-electrode side of the YSZ disk and sintered at 900 °C to create a reference electrode. The reference electrode was placed 3 mm away from the counter electrode.

The current density–voltage characteristics of the anode-supported cell were measured in the temperature range 650–800 °C. Air and 3% humidified hydrogen were supplied as oxidant and fuel, respectively, with flow rates of 30 l/h. The durability of the cathodes was tested using the symmetric cell at 700 °C under air flow of 30 l/h. The tests were conducted for up to 1000 h with a constant current density of 0.2 A cm^{-2} using a three electrodes-four leads geometry.

Detailed microstructure of the cathode was observed by scanning electron microscopy (SEM; ERA-8800FE, Elionix, Japan) and transmission electron microscopy (TEM; JEM-2100F, JEOL, Japan) with energy-dispersive X-ray spectroscopy (EDS; JED-2300T, JEOL, Japan).

3. Results and discussion

Fig. 1 shows the cross-sectional image of the cathode/electrolyte interface of an anode-supported cell. A well-bounded cathode/electrolyte interface can be seen. Successful low-temperature sintering may be attributed to the high surface area of the nano-sized starting particles [13]. The cathode layer consisted of fine, homogeneously connected solid stems and pore channels. Grains approximately 100 nm large were observed.

Fig. 2 shows an STEM image and corresponding EDS mappings of a thin section of the composite cathode. Well-sintered solid stems without significant grain growth may be due to the uniform size and distribution of LSM and YSZ in the starting particles. The average diameter of the solid stems determined from the length of 100 intercepts of randomly drawn lines on the several images was 445 μm, which may represent the size of secondary agglomerates of the composite particles suspended in the screen printing paste [16]. The average diameter of pore channels determined in the same manner was 220 μm. This diameter may be sufficient to diffuse gaseous oxygen, since it was greater than the mean free path of the molecules [17]. The diameter was larger than the grain size. This agrees with the previous studies on sintering, in which pores larger than the grains persist during the densification [18,19]. Porosity estimated from pore area on several TEM images was approximately 25%, and was nearly the optimum value estimated by a computational approach [17]. The distributions of La and Zr in EDS mappings are likely to represent those of LSM and YSZ phases, respectively, since any other phases such as $La_2Zr_2O_7$ and $SrZrO_3$ were not detected in the X-ray diffraction profiles, even when the composite particles were heat treated at 1100 °C [13]. The overlay image of the EDS mappings (Fig. 2(c)) shows that both LSM and YSZ had uniform grain size of about 100 nm and that the uniformly distributed phases were homogeneously connected. Note that many of LSM/YSZ junctions faced the pore channels, suggesting the formation of a large amount of TPBs. This can clearly be attributed to uniformly distributed nano-sized LSM and YSZ grains, in addition to fine and uniformly connected solid stems and pore channels.

Fig. 3 shows the current density–voltage characteristics and the corresponding power density profiles of the anode-supported cell measured between 650 and 800 °C. The open circuit voltage (OCV) was 1.068, 1.064, 1.056 and 1.050 V at 650, 700, 750 and 800 °C, respectively. It was confirmed that the slightly lower OCVs than the theoretical ones (the difference was 0.05–0.06 V) were due to some minor leakage of anode gas through glass sealant. Thus the performance will be slightly underestimated from the real one. Nevertheless, the cells exhibited the high power density

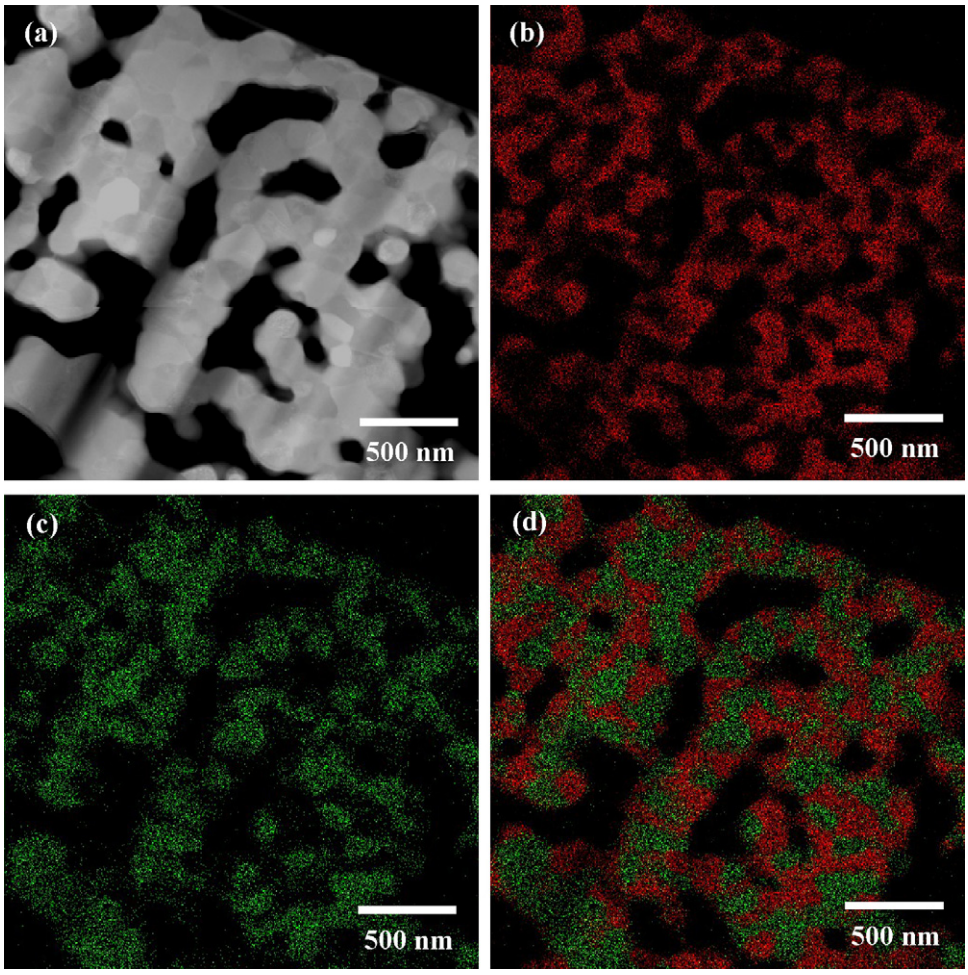

Fig. 2. (a) STEM image, (b) Zr mapping, (c) La mappings, and (d) the overlay image of Zr and La mappings of a nanostructured cathode.

of 0.20, 0.40, 0.69 and 0.85 W cm^{-2} at 650, 700, 750 and 800 °C, respectively, under the cell voltage of 0.7 V. This high performance indicates that the anode-supported cell with the present nanostructured cathode has potential to be operated at the intermediate temperature range with an acceptable power density. Clearly, the high performance can be attributed to the formation of a large amount of TPBs in the nanostructured cathode. The performance was better than that of the cells with a $La_{0.6}Sr_{0.4}Co_{0.2}Fe_{0.8}O_{3-\delta}$ (LSCF) cathode fabricated under optimized processing conditions [14,20]. Materials and processing parameters of the present thin-film YSZ electrolyte and Ni/YSZ anode, as well as the testing conditions were the same as in the previous studies. In the common sense, LSCF has superior ORR property to LSM/YSZ composite at intermediate temperature. However these facts indicated that the present nanostructured LSM/YSZ cathode has better ORR property than the LSCF cathode. The electrochemical performance of the composite cathode is no longer the bottleneck of the overall cell performance, since that of Ni/YSZ anode limited the overall performance of the cell with the LSCF cathode [14].

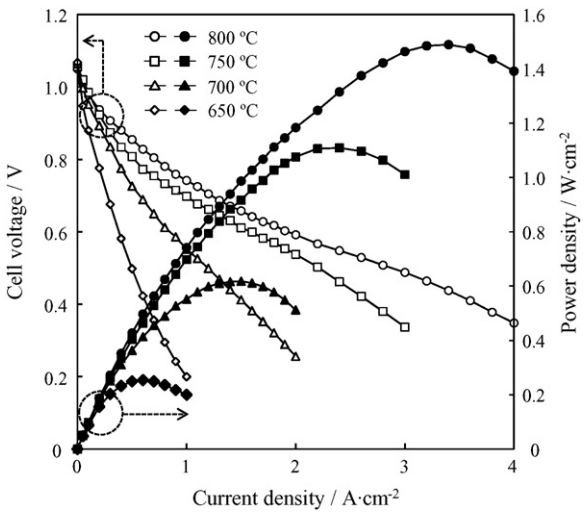

Fig. 3. Current density–voltage characteristics and corresponding power density profiles of the anode-supported cell measured between 650 and 800 °C.

Fig. 4 shows the polarization of a nanostructured LSM/YSZ cathode as a function of operation time measured using the symmetric cell at 700 °C under a current load of 0.2 A cm^{-2}. In this condition, the anode-supported cell with the nanostructured cathode can be operated at an acceptable power density of 0.2 W cm^{-2} under cell voltages above 0.8 V, as shown in Fig. 3. The cathode exhibited good long-term performance stability under the test condition. The polarization after 1000 h was almost the same as at the beginning, even though the presence of some minor perturbations which probably due to some changes in the experimental conditions such as local temperature and humidity of supplied air. Liu et al. suggest that the formation of zirconates at the cathode/electrolyte interface was responsible for the performance degradation of the cathode, and their formation can be related to the chemical instability of

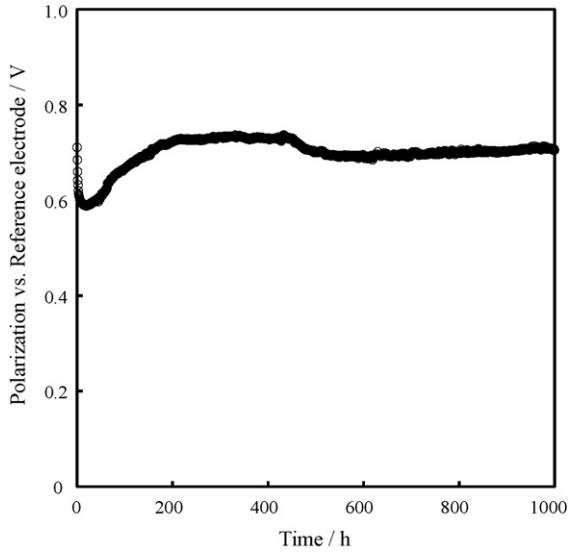

Fig. 4. Polarization of the cathode vs time under a constant current density of 0.2 A cm^{-2} at 700 °C.

LSM under a current load [11]. They estimate the risk of zirconate formation as a function of oxygen partial pressure at the interface ($p(O_{2,Interface})$) based on a thermodynamic model. The value of $p(O_{2,Interface})$ during operation can be estimated by the Nernst equation as a function of cathodic polarization and temperature [11]. Polarization of the present nanostructured LSM/YSZ cathode extracted from the total polarization of the symmetric cell using the current interruption technique [14,20] was 0.17 V at the initial stage of testing. The calculated $p(O_{2,Interface})$ was 6.30×10^{-5} atm, and is high enough to avoid the formation of zirconates at 700 °C [11].

Fig. 5 shows an SEM image of the cathode after a durability test. Although grain size stayed constant, the morphology of individual grains changed after testing. Jiang et al. reported a similar morphological change on an A-site deficient LSM cathode under a current load [21]. They reported that the morphological change causes a drastic reduction of cathodic polarization during the initial stage, as shown in Fig. 4. They suggested a possible mechanism

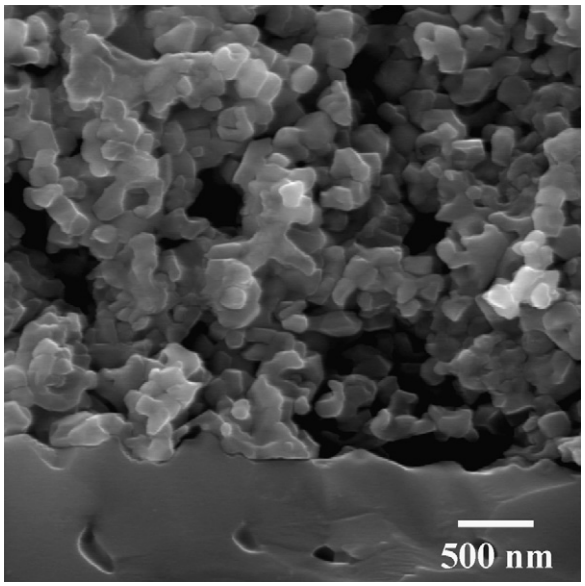

Fig. 5. A cross-sectional SEM image of the cathode/electrolyte interface after durability testing.

of the morphological change via significant generation and migration of oxygen vacancies and manganese ions on the surface and along the grain boundaries of LSM. These could weaken the contact between particles, leading to disintegration of agglomerates in the case of A-site deficient LSM. Similar phenomena may occur in the present nanostructured cathode, since the LSM in the present study is also A-site deficient. Nevertheless, despite the morphological change by surface and grain boundary diffusion, grain size remained nearly constant. This may be due to the suppression of grain boundary migration by a uniformly distributed YSZ phase within the cathode, as shown in Fig. 2. Some small cracks were observed at the cathode/electrolyte interface. Liu et al. reported that these cracks were formed due to the formation of zirconates during operation [11]. However, the analysis of a local area by SEM-EDS could not show conclusive evidence of zirconate formation. In addition, the $p(O_{2,Interface})$ was kept sufficiently high to suppress their formation, as discussed above. Further analysis is needed to clarify the detailed mechanism of formation of the local cracks. However, if we assumed that the increase in the polarization between 20 and 200 h was caused by the formation of these cracks, the constant polarization up to 1000 h suggested that they did not extend during the entire period. In summary, the present high-performance nanostructured cathodes can enhance long-term performance stability of IT-SOFCs not only by minimizing zirconate formation and crack extension at the cathode/electrolyte interface, but also by maintaining considerable amount of TPBs.

4. Conclusions

Nanostructured LSM/YSZ cathodes with fine and uniformly connected LSM, YSZ and pore phases formed a large amount of the TPBs, giving rise to high-performance IT-SOFCs. Such a high-performance nanostructured cathode can enhance the long-term performance stability by suppressing zirconate formation, crack extension and grain growth during operation. The present nanostructured LSM/YSZ is a promising cathode material for IT-SOFCs.

Acknowledgements

This work was partly supported by a Scientific Research Grant from the Ministry of Education, Science, Sports, and Culture of Japan.

References

[1] J.M. Ralph, A.C. Schoeler, M. Krumpelt, J. Mater. Sci. 36 (2001) 1161–1172.
[2] T. Kenjo, M. Nishiya, Solid State Ionics 57 (1992) 295–302.
[3] K. Sasaki, J.-P. Wurth, R. Gschwend, M. Gödickemeier, L.J. Gauckler, J. Electrochem. Soc. 143 (1996) 530–543.
[4] F.H. van Heuveln, H.J.M. Bouwmeester, F.P.F. van Berkel, J. Electrochem. Soc. 144 (1997) 126–133.
[5] J. Piao, K. Suna, N. Zhang, S. Xub, J. Power Sources 175 (2008) 288–295.
[6] J.-H. Kim, R.-H. Song, J.-H. Kim, T.-G. Lim, T.-K. Sun, D.-R. Shin, J. Solid State Electrochem. 11 (2007) 1385–1390.
[7] M. Mamak, G.S. Métraux, S. Petrov, N. Coombs, G.A. Ozin, M.A. Grees, J. Am. Chem. Soc. 125 (2003) 5161–5175.
[8] H.S. Song, S. Lee, S.H. Hyun, J. Kim, H.-W. Lee, J. Moon, J. Mater. Chem. 18 (2008) 1087–1092.
[9] W.G. Wang, Y.-L. Liu, R. Barfod, S.B. Schougaard, P. Gordes, S. Ramousse, P.V. Hendriksen, M. Mogensen, Electrochem. Solid-State Lett. 8 (2005) A619–A621.
[10] A. Hagen, R. Barfod, P.V. Handriksen, Y.-L. Liu, S. Ramousse, J. Electrochem. Soc. 153 (2006) A1165–A1171.
[11] Y.L. Liu, A. Hagen, R. Barfod, M. Chen, H.J. Wang, F.W. Poulsen, P.V. Hendriksen, Solid Sate Ionics 180 (2009) 1298–1304.
[12] A. Hagen, Y.L. Liu, R. Barford, P.V. Hendriksen, J. Electrochem. Soc. 155 (2008) B1047–B1052.
[13] K. Sato, T. Kinoshita, H. Abe, M. Naito, J. Ceram. Soc., Jpn. 117 (2009) 1186–1190.

[14] H. Abe, K. Murata, T. Fukui, W.-J. Moon, K. Kaneko, M. Naito, Thin Solid Films 496 (2006) 49–52.
[15] K. Sato, G. Okamoto, H. Abe, M. Naito, ECS Trans. 7 (2007) 1555–1561.
[16] A. Hagiwara, N. Hobara, K. Takizawa, K. Sato, H. Abe, M. Naito, Solid State Ionics 178 (2007) 1123–1134.
[17] R.E. Williford, P. Singh, J. Power Sources 128 (2004) 45–53.
[18] F.F. Lange, B.J. Kellet, J. Am. Ceram. Soc. 72 (1989) 735–741.
[19] W.D. Kingery, B. Francois, in: G.C. Kuczynski, N.A. Hooton, G.N. Gibbon (Eds.), Sintering and Related Phenomena, Gordon and Breach, New York, 1967, pp. 471–498.
[20] K. Murata, T. Fukui, H. Abe, M. Naito, K. Nogi, J. Power Sources 145 (2005) 257–261.
[21] S.P. Jiang, J.G. Love, Solid State Ionics 158 (2003) 45–53.